Original Article

NHERF1/EBP50 immunoexpression in renal cell carcinomas and oncocytomas with ultrastructural analysis of clear cell renal cell carcinoma

Aliaksandr Aksionau[1]^, Roberto A. Silva[1], Brandon Hartman[2], Ashley Flowers[1]^

[1]Department of Pathology and Translational Pathobiology, LSU Health Shreveport, Shreveport, LA, USA; [2]Department of Pathology, Ochsner LSU Health, Shreveport, LA, USA

Contributions: (I) Concept and design: A Aksionau, RA Silva, A Flowers; (II) Administrative support: A Aksionau, A Flowers; (III) Provision of study materials or patients: A Aksionau, A Flowers; (IV) Collection and assembly of data: A Aksionau, A Flowers; (V) Data analysis and interpretation: A Aksionau, B Hartman, A Flowers; (VI) Manuscript writing: All authors; (VII) Final approval of manuscript: All authors.

Correspondence to: Aliaksandr Aksionau, MD. Department of Pathology and Translational Pathobiology, LSU Health Shreveport, 1501 Kings Hwy, Shreveport, 71103 LA, USA. Email: aliaksandr.aksionau@emory.edu.

Background: Na^+/H^+ exchanger (NHE) maintains the alkaline pH of epithelial cells working at the cellular membrane and exchanging H^+/Na^+ ions. In renal tubular epithelial cells, the reabsorption of NaCl is implemented by NHE3 isoform, which is regulated by NHE regulatory factor-1 (NHERF1). Normally situated at the apical zones of proximal tubular cells, NHERF1 participates in cytoskeletal reorganization and signal transduction facilitating structural stability and ion exchange. Based on an extensive search in English literature, NHERF1/EBP50 immunoexpression has been studied in breast, colon, and other tumors with only one study on 21 cases of renal cell carcinomas (RCC).

Methods: Using NHERF1/EBP50 immunohistochemistry (IHC) on 64 (82%) RCCs (34 clear cells, 21 papillary and 9 chromophobe types) and 14 (18%) oncocytomas, we evaluated and scored NHERF1/EBP50 immunoexpression depending on the World Health Organization (WHO)/International Society of Urological Pathology (ISUP) grading system followed by ultrastructural identification of microlumen-like structures (MLS) in clear cell renal cell carcinomas (ccRCC).

Results: Staining patterns varied throughout the tumors and within individual tumors. Only ccRCC showed unique MLS within the cytoplasm of tumor cells. All neoplasia-transformed tubular cells, regardless of the tumor grade and stage, had altered immunoexpression of NHERF1/EBP50 ranging from complete absence to aberrant expression in the luminal cell membrane, nuclear or cytoplasmic localizations.

Conclusions: Only ccRCC showed unique dot-like condensations of immunostaining/MLS at membranous, submembranous, and paranuclear localizations. The latter two localizations were mainly observed in the combined WHO/ISUP grade 1 and 2 group compared to the combined group of grade 3 and 4 tumor samples ($P=0.0146$ and $P<0.0001$, respectively). Ultrastructurally, the MLS were identified as thick microvilli trapped by a single-layer membrane, displaced into the cytoplasm and ranging from 400 nm to 3.5 µm. These significant ultrastructural reorganizations may contribute to tumor progression, metastasis, and drug resistance.

Keywords: NHERF1/EBP50; renal cell carcinoma (RCC); oncocytoma; electron microscopy; microlumen

Submitted Feb 16, 2023. Accepted for publication Jul 07, 2023. Published online Aug 14, 2023.
doi: 10.21037/tau-23-101
View this article at: https://dx.doi.org/10.21037/tau-23-101

^ ORCID: Aliaksandr Aksionau, 0000-0003-0741-2000; Ashley Flowers, 0000-0002-9030-2971.

Introduction

Annually, the American Cancer Society estimates the number of new cancer cases and deaths in the United States. For kidney and renal pelvis cancer, the projected increase in new cases is approximately 4.1%, with an estimated rise of 2.3% in deaths. The overall ratio for new cases among women and men is estimated at 1:0.6; the same numbers are set for deaths (1). Worldwide, renal cell carcinoma (RCC) represents the 6th most frequently diagnosed cancer in men and the 10th in women (2). According to 2019 statistics, kidney and renal pelvis cancer ranked 5th in importance among the causes of death of women under 20 years of age (1).

Renal epithelial tumors such as clear cell, papillary, chromophobe RCC, and oncocytoma are most common among primary renal epithelial neoplasms. Of these, RCCs accounts approximately 85–90% of all primary renal cancers (3,4). Clear cell RCC subtype (ccRCC) accounts for 65–70% of all renal cancers, can be familial or sporadic, and is typically characterized by loss of the short arm of chromosome 3 (-3p) (3). The key role in oncogenesis is the inactivation/loss of the von Hippel Lindau tumor suppressor gene (5,6).

Based on the function and ultrastructural characteristics, the proximal tubule of the nephron can be divided into S_1, S_2, and S_3 segments (7,8). The most distinctive feature of S_1 cells is the extensive specialization (dense brush border and intercellular interdigitations) of their apical membranes, the site of the greatest functional activity (7,9). Apical membranes contain Na^+/H^+-antiporters, also known as Na^+/H^+ exchangers (NHE), which participate in luminal Na^+ entry into proximal tubular cells from the apical membranes (9-11). NHE exchanges one intracellular H^+ ion for one extracellular Na^+ ion, maintaining the necessary intracellular alkaline pH balance (10). Several types of NHE have been described with a predilection for one or another type of epithelial cells.

NHE3 is a major Na^+ transporter in the luminal membrane of the proximal tubules (12). Na^+/H^+ exchanger regulatory cofactor 1 (NHERF1) is one of the cofactors that regulates the activity of NHE3. The association between NHE3 and NHERF1 appears to occur within the cell membrane (13,14). It stabilizes the organization of the actin skeleton, formation of tight junctions, protein targeting, microvilli formation, and assembly of protein complexes (15). It is known that mice lacking NHERF1 have been shown to have short aberrant microvilli (16). Recent studies revealed the involvement of NHERF1 in a variety of intracellular functions across multiple cell lines. The list is incomplete and includes processes associated with inflammatory response, tissue injury, cell structure and trafficking, tumorigenesis, and tumor behavior (15,17).

The expression and regulation of NHERF1 have been comprehensively studied in various tumors (breast, colon, uterine cervix, etc.), as well as its possible role on the effects of chemotherapeutic drugs (18,19). The results showed emerging evidence of altered expression associated with tumor behavior. Secretory and chordoid meningiomas showed microvillar interdigitations with microlumen-like NHERF1/EPB50 positive immunostaining (20). Located on apical cell membranes, NHERF1 acts as a tumor suppressor and becomes a pro-oncogene when it relocates into the cytoplasm or nucleus (21,22).

A comprehensive literature search has revealed a study of NHERF1/EBP50 immunoexpression in 21 cases of RCC [15 cases of ccRCC, 5 cases of chromophobe RCC (chrRCC) and 1 case of mixed RCC tumor] using light microscopy only (23).

We decided to expand the list by examining oncocytomas and the three most common types of RCC. Using NHERF1/EBP50 immunohistochemistry (IHC), we aimed to identify NHERF1-associated pathomorphological changes with association with the neoplastic process, comparing selected tumors with each other and benign renal parenchyma, suggesting the use of electron microscopy in

Highlight box

Key findings

- NHERF1/EBP50 immunoexpression appears abnormal in studied clear cell, papillary, and chromophobe types of renal cell carcinomas and oncocytomas.
- Microlumen-like structures highlighted by NHERF1/EBP50 appear to be unique to clear cell renal cell carcinoma among the other most common renal tubular epithelial tumors.
- These structures are microvilli trapped by a single-layer membrane, ranging from 400 nm to 3.5 µm, and relocated from the cell membrane into the cytoplasm.

What is known and what is new?

- To the best of our knowledge, microlumen-like structures has not been previously described in renal cell oncology.
- Our results may shed more light on pathogenesis of kidney tumors.

What is the implication, and what should change now?

- Our findings may help understand oncogenesis, stimulate additional research, and open up new therapeutic possibilities in renal oncology.

case of finding unique results.

A total of 14 (18%) oncocytomas and 64 (82%) RCCs were analyzed [ccRCC, papillary RCC (pRCC) and chrRCC types were represented by 34 (44%), 21 (27%) and 9 (11%) cases, respectively]. Our results were derived from light microscopy and ultrastructural analysis findings. Abnormal NHERF1/EBP50 immunoexpression (meaning other than diffuse cytoplasmic and strong linear luminal of renal tubular epithelial cells) was seen in most of the studied tumor types [69 (88%) cases]. We assessed the association of expression with the grade and stage of the tumor, the presence or absence of necrosis, and localization in the cell. We found that only ccRCC showed formation of unique NHERF1/EBP50 condensations/microlumen-like structures (MLS). The last twelve cases of ccRCC were subjected to a broader analysis including transmission electron microscopy (TEM). NHERF1/EBP50 condensations appeared in the form of membranous, submembranous, and paranuclear aggregates/well-outlined clusters of thick microvilli trapped by a single-layer membrane and ranging from hundreds of nanometers to several micrometers in the greatest dimension.

Although ccRCC is a well-known tumor with current treatment options available, its oncogenesis differs significantly from that of other kidney tumors, and the exact oncogenesis is not fully understood. We aim to deepen this understanding by characterizing the immunohistochemical expression of NHERF1/EBP50 and how it is associated with grade and stage of RCC. We present this article in accordance with the STROBE reporting checklist (available at https://tau.amegroups.com/article/view/10.21037/tau-23-101/rc).

Methods

Case selection and tissue preparation

The study was conducted in accordance with the Declaration of Helsinki (as revised in 2013). The current study was approved by the Institutional Review Board Committee at LSU Health Shreveport (No. CR00002192_STUDY00000740) and individual consent for this retrospective analysis was waived.

Primarily, all the cases managed by the department were sequentially included in the study with no exclusion. First of all, we performed a retrospective search using our pathology database for all renal epithelial tumors managed by the department from 2010 to 2019. A total of 66 cases of renal tumors were selected including 14 cases of oncocytoma and 52 cases of RCC [ccRCC, pRCC, and chrRCC were represented by 22 (42%), 21 (40%) and 9 (17%) cases, respectively]. Using stored formalin-fixed and paraffin-embedded tissue blocks (in the ratio of one block per case), 4-microns tumor tissue sections were immunostained with NHERF1/EBP50 [polyclonal rabbit IgG antibodies (1:3,000 dilution) to ezrin-radixin-moesin (ERM) binding phosphoprotein (ThermoFisher Scientific, Waltham, Massachusetts, USA)] followed by an assessment of localization and expression pattern. The combination of membranous (luminal, strong and linear) with cytoplasmic (weak, diffuse) patterns of immunostaining of renal tubular epithelial cells were considered as normal (24). Other types of immunoexpression (its complete absence or nuclear and/or patchy cytoplasmic with/or without membranous) were considered abnormal (*Table 1*).

All primarily studied cases were found to have one or another type of abnormal NHERF1/EBP50 immunoexpression. Additionally, nine cases of ccRCC showed formation of unique MLS in the cytoplasm. Considering the finding above, it was decided to obtain additional ccRCC cases specifically to identify tumors with MLS and analyze these structures by TEM. From 2019 to 2021, all new kidney tumors received by the department were considered as potential cases of ccRCC. Only if the volume of tumor tissue allowed, three samples of fresh tumor were taken from heterogeneous sites of each new tumor in order to find sites with MLS. Of the 19 new cases with suspected ccRCC, only 12 were diagnosed as ccRCC, the remaining types of kidney tumors were rejected (*Table 2*).

Since tumors were histologically heterogeneous and expression of NHERF1/EBP50 varied through the tumors, we needed a method to select areas for ultrastructural evaluation after IHC performed. In order to prospectively determine which tumor samples will require subsequent TEM evaluation, we have developed a unique system for mapping tumor specimens. While main samples were used for IHC, the secondary samples were appropriately stored for possible ultrastructural evaluation if the main tumor sample revealed MLS by previous IHC analysis. To be more efficient, these three main samples were cut rectangular (approximately 1.0×0.7×0.3 cm^3) with small secondary samples (approximately 0.6 to 0.3×0.3×0.3 cm^3) taken from each main sample in the form of an irregular triangle (secondary sample "A"), a right triangle (secondary sample "B") and a rectangle (secondary sample "C") (*Figure 1A*). This helped us to identify the main samples and allowed us to place all three main samples in the same

Table 1 Characteristics of NHERF1/EBP50 immunoexpression in 14 oncocytomas and 52 initially analyzed RCCs

Tumor type	Number of cases	NHERF1/EBP50 immunoexpression in tumor cells (number of cases)										
		Completely negative	Pure membranous	Membranous +				Pure cytoplasmic		Pure nuclear	Overall pattern of staining	
				+ Cytoplasmic		+ Cytoplasmic & nuclear						
				Diffuse/ patchy	Lumen-like	Diffuse/ patchy	Lumen-like	Diffuse/ patchy	Lumen-like		Heterogeneous	Homogeneous
ccRCC	22	0	5	7	9	1	0	0	0	0	12	10
pRCC												
Type I	13	0	4	6	0	2	0	1	0	0	7	6
Type II	8	1	0	5	0	0	0	2	0	0	1	6
chrRCC	9	7	0	1	0	0	0	1	0	0	2	0
Oncocytoma	14	2	0	11	0	0	0	1	0	0	2	10

+, means adding another extra pattern/patterns of expression. NHERF1, Na+/H+ exchanger regulatory cofactor 1; RCC, renal cell carcinoma; ccRCC, clear cell renal cell carcinoma; pRCC, papillary renal cell carcinoma; chrRCC, chromophobe renal cell carcinoma.

Table 2 Characteristics of 12 additional cases of clear cell RCC

Case[#]	Gender	Age (years)	Stage	Side	Size (the greatest dimension, cm)	Focality	WHO/ISUP nuclear grade	Necrosis	Type of surgery	Regional lymph node status (# positive/# submitted or found)
1[†]	M	51	pT2a	Lt	7.3	Uf	3	+	ORN	0/0
2[†]	M	62	pT3a	Rt	7	Uf	2	+	ORN	0/0
3[†]	M	48	pT1b	Rt	5.5	Uf	2	–	ORN	0/0
4	M	43	pT1a	Lt	2.6	Uf	3	+	RPN	0/0
5[¶]	M	50	pT3a	Lt	10	Uf	3	+	ORN	0/0
6[$]	M	58	pT3a	Lt	7	Uf	4	+	ORN	0/17
7[†]	M	38	pT3a	Rt	9.6	Mf	3	–	ORN	0/2
8[†]	M	51	pT2a	Lt	8	Uf	3	–	ORN	0/35
9[†]	F	64	pT3a	Rt	5	Uf	3	–	RTN	0/0
10	F	30	pT1a	Lt	3.7	Uf	3	+	RPN[§]	0/0
11[†]	F	52	pT1a	Lt	2.5	Uf	1	–	RPN	0/1
12	M	68	pT1b	Lt	4.2	Uf	2	–	RPN[§]	0/0

[#], number; [†], selected for transmission electron microscopy; [¶], histologically confirmed metastatic disease at the time of diagnosis; [$], sarcomatoid features present; [§], surgical margin of resection was focally positive for tumor cells. RCC, renal cell carcinoma; WHO/ISUP, World Health Organization/International Society of Urological Pathology; M, male; F, female; Lt, left-sided; Rt, right-sided; Uf, unifocal; Mf, multifocal; +, present; –, absent; ORN, open radical nephrectomy; RPN, robotic partial nephrectomy; RTN, robotic total nephrectomy.

cassette for fixation in a 10% buffered formalin solution and subsequent processing (*Figure 1B*). Geometrically different secondary samples were separately placed in a container with 2.5% glutaraldehyde solution for possible future TEM (*Figure 1C*). The containers were stored in the refrigerator at a temperature of +4 ℃. Our method has helped to reduce the workload on our histology laboratory and reduce costs, while also maintaining a map between tumor areas with MLS identified by NHERF1/EBP50 IHC with tumor areas most likely to have MLS in the TEM sample.

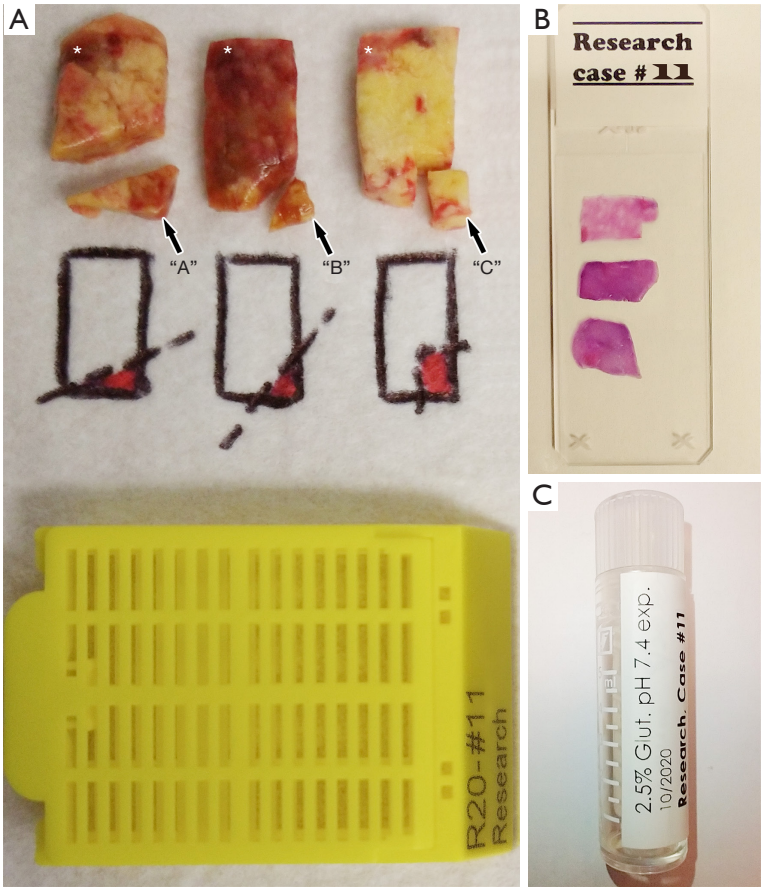

Figure 1 Sample processing. (A) Both main samples (marked with asterisks) and secondary samples (indicated by arrows with notations) are meticulously selected from grossly heterogeneous regions within the same tumor. (B) The accompanying photograph illustrates the visual representation of the main samples on a glass slide subsequent to histological processing. (C) The corresponding secondary samples are stored in a single container containing a 2.5% glutaraldehyde solution at pH 7.4.

For the newly formed group of twelve ccRCC, 12 cassettes with new main samples (3 samples per tumor, 36 samples in total) were transferred to histology for embedding and histological processing. The tumor sections were stained with hematoxylin-eosin (H&E) and immunostained with NHERF1/EBP50.

Using light microscopy, all samples were confirmed as ccRCC (25). The corresponding immunostained tissue sections were analyzed and scored for the presence of NHERF1/EBP50 immunoexpression with respect to tumor viability, World Health Organization (WHO)/International Society of Urological Pathology (ISUP) nuclear grade, and tumor stage (*Figure 2A-2D*) (26). Several cases that were previously assessed using the Furman scoring system were re-assessed using the WHO/ISUP scoring system.

For ultrastructural analysis, 9 minor tissue samples were selected. This selection was made with respect to the corresponding main samples showing the most evidence of MLS with NHERF1/EBP50 immunostaining.

Material processing and IHC

All tumor samples were formalin-fixed and paraffin-embedded. 4-microns tissue sections were stained routinely with H&E and immunostained with NHERF1/EBP50 [polyclonal rabbit IgG antibodies (1:3,000 dilution) to ERM binding phosphoprotein (ThermoFisher Scientific, Waltham, Massachusetts)]. For immunohistochemical staining, paraffin-embedded sections were incubated in the Fisher Scientific oven at 75 ℃ for 30 minutes and

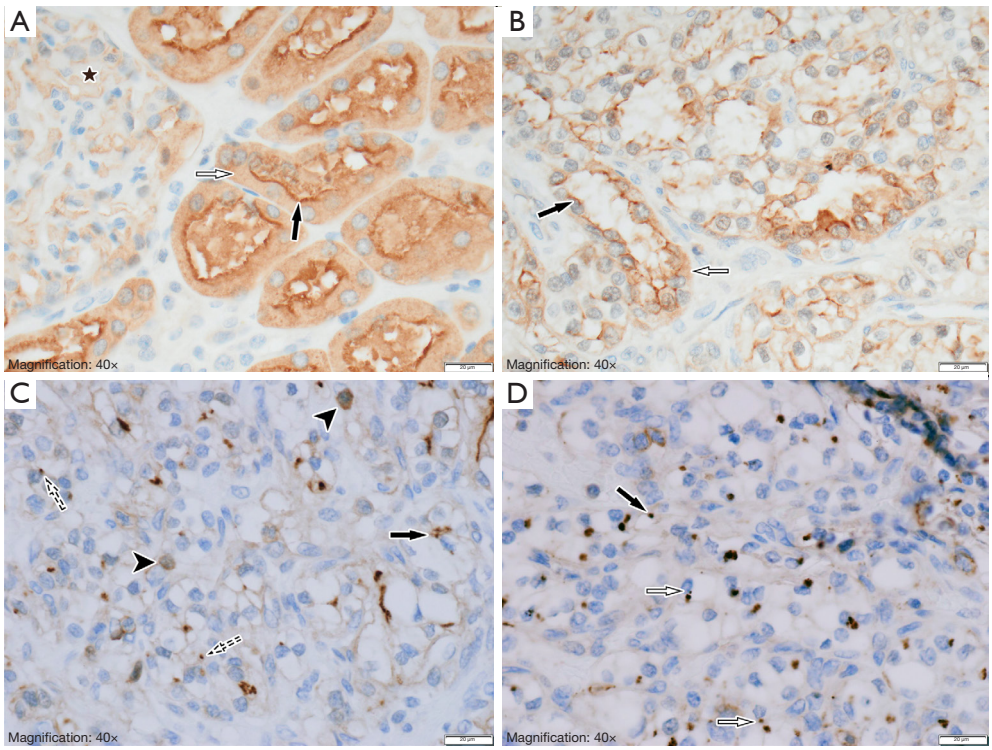

Figure 2 NHERF1/EBP50 immunoexpression findings on light microscopy. (A) Within the benign renal parenchyma, proximal tubular epithelial cells demonstrate strong and linear luminal NHERF1/EBP50 immunoexpression (indicated by a black arrow), while cytoplasmic expression appears diffuse and weak (indicated by a white arrow). Glomerular podocytes (marked with an asterisk) exhibit focal and weak NHERF1/EBP50 immunopositivity. (B) In areas where clear cell renal cell carcinoma cells form tubules, NHERF1/EBP50 immunoexpression is comparable to the benign renal parenchyma, albeit with reduced intensity (luminal and cytoplasmic expression is denoted by black and white arrows, respectively). (C,D) Immunostaining of NHERF1/EBP50 in ccRCC cells reveals noteworthy condensations/microlumen-like structures in membranous (indicated by dashed arrows), submembranous (indicated by black arrows), and paranuclear (indicated by white arrows) localizations. Infrequently, weak NHERF1/EBP50 immunopositivity is observed in tumor cell nuclei (marked by arrowheads). (NHERF1/EBP50 immunostaining, 40×). NHERF1, Na+/H+ exchanger regulatory cofactor 1; ccRCC, clear cell renal cell carcinoma.

subsequently processed with Roche Diagnostics Ventana BenchMark Ultra Slide Stainer.

Light microscopy and tissue assessment

Hematoxylin and eosin-stained main samples from 12 ccRCC cases were qualitative analyzed in percent, including the presence of a solid tumor component, necrosis, a cystic/hemorrhagic component and, if present, benign renal parenchyma. The latter, if present on the slide, served as an internal control for NHERF1/EBP50 immunostaining in addition to the external control tissue.

The intensity of NHERF1/EBP50 immunoexpression was evaluated in areas of maximal expression ("hot-spot") semi-quantitatively compared to the control tissue. Four ordinal variables from zero [0] to three [3] were used: 0 – no expression, 1 – weak, 2 – moderate, and 3 – strong.

Localization of NHERF1/EBP50 immunoexpression was evaluated on the cell membrane, cytoplasm, and nucleus. Using two categorical variables, we analyzed the presence or absence of MLS in the membranous, submembranous, and paranuclear regions as absent or present. If present, the density was estimated on a high-power field (40×) using four ordinal variables in combination with a categorical variable as follows: 1+ (one MLS present), 2+ (from 2 to 3 MLS present) and 3+ (≥4 MLS present). In addition, this assessment was carried out in relation to the WHO/ISUP nuclear grading system of the tumor cells.

TEM

Using selected 11 secondary samples (from 9 ccRCC), thin slices of tissue were fixed in formaldehyde for a minimum of 4 hours. Each specimen was inspected and dissected for the most suitable tissue with fragments below 3 mm in length needed for EM microscopy. The specimens were transferred to 1% OsO_4 for approximately 45 minutes. They were then dehydrated through a graded alcohol series and gradually infiltrated with series of resin to acetone mixtures. Specimens were then embedded in a PELCO embedding mold with a pre-trimmed end and placed in an oven overnight. Thin (80 nm) sections were cut from each specimen block with an ultra-45 diamond knife and placed on 200 mesh copper grids. Sections were photographed with a JEOL TEM-1400 transmission electron microscope with Advanced Microscopy Techniques imaging software. Each section of the grid was fully examined for the presence of MLS or any unusual structures.

Statistical analysis

Descriptive statistics were used. For measured variables, medians and ranges were calculated. For categorical variables, frequency counts and percentages were used. For statistical significance, attributable risks were calculated using a two-sided Fisher's exact test. P values <0.05 were considered statistically significant. The figures were created using GraphPad Prism v.8 software. Microsoft Office Excel 2016 was used to create tables. Adobe Photoshop CS6 software was used to process images and create figures.

Results

Demographic characteristics and clinical findings

A total of 14 oncocytomas and 64 RCCs were studied during the entire project, which were immunostained with NHERF1/EBP50. Among cases of RCC, clear cell, papillary, and chromophobe types were represented by 34 (53%), 21 (33%), and 9 (14%) cases, respectively.

Among the latter group of 12 ccRCC cases, the mean age was 51.8±2.1 years, with the youngest and oldest patients being 30 and 75 years old, respectively. The ratio of women and men was 1:3. The mean tumor size was 6.2±0.6 cm. WHO/ISUP nuclear grade 3 was the most frequent [7 (58%) cases]. pT3a was the dominant tumor stage, accounting for 5 (42%) cases. Necrosis was noted in 6 (50%) cases. None of the lesions had a rhabdoid morphology, and only one case had sarcomatoid features (*Table 2*). In the nephrectomy specimen of patient #7, two tumor nodes were identified [9.6×8.5×6.9 cm^3 (lower half) and 1.8×1.2×1.2 cm^3 (superior pole)]. Despite being multifocal, there was no family history of von Hippel-Lindau syndrome, and the patient had no other lesions associated with it, so genetic testing was not performed. Only patient #5 with the largest tumor nodule was known to have a metastatic disease to the lung prior to surgery, which was confirmed histologically. All submitted/found lymph nodes were free of tumor cells. Only in two patients (#10 and #11) surgical resection margins were focally positive for carcinoma (robotic partial nephrectomies were done in both cases). Patient #11 was lost to follow-up, and patient #10 stayed free of disease recurrence 2.9 years after surgery (based on March 2023).

Assessment of H&E and NHERF1/EBP50 stained slides

The initial evaluation of tumor samples by light microscopy confirmed that they were consistent with the tumor types identified in the final surgical reports (25,27).

For the initial group of 14 oncocytomas and 52 RCCs, NHERF1/EBP50 immunoexpression was analyzed in membrane, cytoplasmic, and nuclear locations. The combination of membranous (luminal, strong and linear) and cytoplasmic (weak, diffuse) patterns of NHERF1/EBP40 immunostaining of renal tubular epithelium was considered normal based on the scientific literature (24). This staining pattern was detected in 9 (14%) cases (5 ccRCC and 4 pRCC type I). In the remaining 57 (86%) cases, one or another type of abnormal immunoexpression was detected (complete absence or nuclear and/or patchy cytoplasmic with/or without membranous immunostaining). Heterogeneity of immunoexpression was observed among all the tumor types studied and within individual tumors, regardless of grade and stage. However, MLSs highlighted by NHERF1/EBP50 were detected only in 9 (14%) cases related to ccRCC (*Figure 2C,2D*).

A comprehensive evaluation of 36 main samples collected (from an additional 12 ccRCC cases) showed that all four components (solid tumor, benign renal parenchyma, necrosis and hemorrhagic/cystic component of the tumor) were detected in 6 (18%) samples.

NHERF1/EBP50 immunoexpression in tumor cells (membranous, cytoplasmic, and nuclear levels) was variable in all tumors and within the same tumor, depending on the WHO/ISUP nuclear grade and tumor stage. This confirmed the primarily established results obtained in

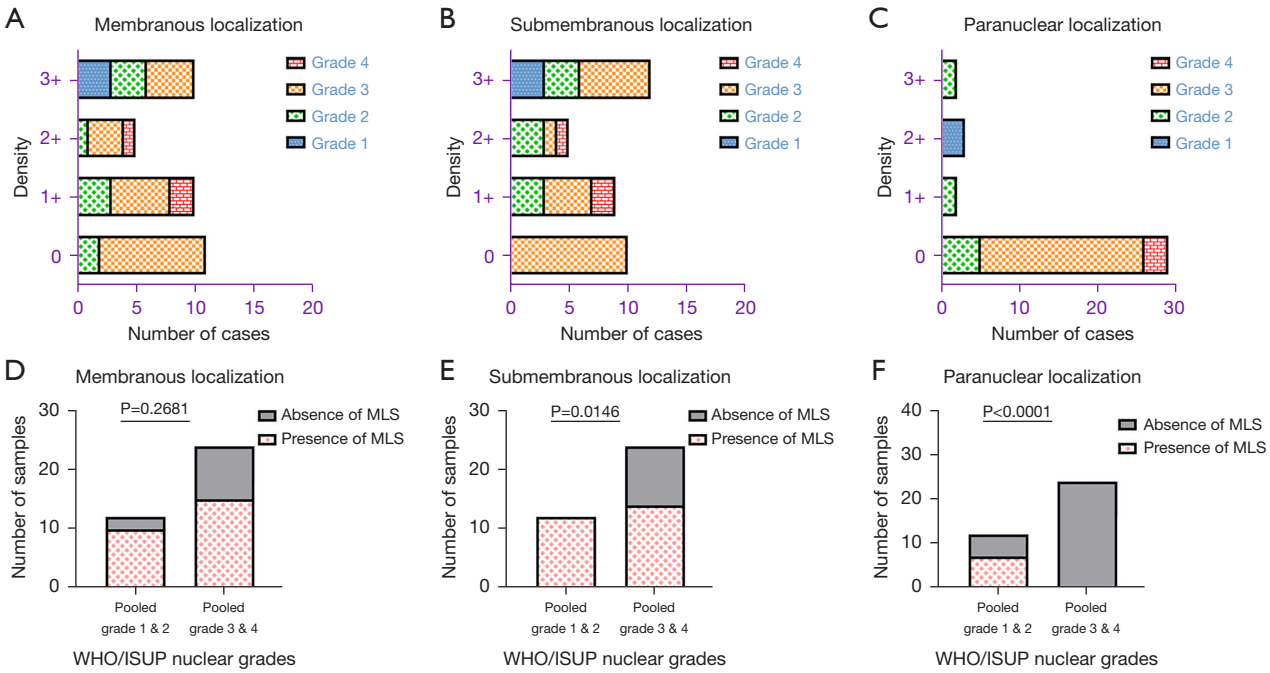

Figure 3 Density of microlumen-like structures with statistical analysis on the main 36 samples of 12 ccRCC cases. (A-C) MLS density in membranous, submembranous, and paranuclear localizations, respectively. (D-F) Comparison of MLS formation between tumors with WHO/ISUP grade 1 and 2 and those with grade 3 and 4, specifically in membranous, submembranous, and paranuclear sites, respectively. ccRCC, clear cell renal cell carcinoma; MLS, microlumen; WHO/ISUP, World Health Organization/International Society of Urological Pathology.

the study of oncocytomas and RCC. Normal expression was found in samples where tumor cells formed tubular structures with a preserved brush border (*Figure 2B*).

Since the number of tumor samples obtained from the last 12 cases of ccRCC was small for statistical analysis, it was decided to combine nuclear grade 1 and 2 tumor samples into the "low-grade group", and the nuclear grade 3 and 4 tumor samples into the "high-grade group".

MLSs have been identified in the membranous, submembranous, and paranuclear localizations. Statistically, the latter two were most frequently observed in tumor samples from the low-grade group (0.4167; 95% CI: 0.0612 to 0.6307; P=0.0146 and 0.5833; 95% CI: 0.24 to 0.8350; P<0.0001, respectively). In the high-grade group, paranuclear localization of MLS was not observed in any of the studied samples (*Figure 3A-3F*). The proximity of tumor cells to the zone of necrosis significantly affected the formation of MLS; they were rarely observed at the membrane and were completely absent in the submembranous and/or paranuclear localizations (*Table 3*).

It is important to note that MLS has not been observed in adjacent benign renal parenchyma.

Ultrastructural analysis findings

Out of thirty-six, the eleven main samples showed the most prominent MLS highlighted by NHERF1/EBP50 IHC; the corresponding secondary samples were subjected to ultrastructural analysis. MLS were thick microvilli surrounded by a single-layer membrane. They ranged in diameter from 400 nm to 3.5 µm and were located in the membranous, submembranous, and paranuclear regions (*Figures 4A-4D,5A-5D*). The membranous arrangement appeared to be brush border microvilli trapped between two adjacent tumor cells (cell membranes extending from MLS were visible). Submembranous MLS in some cases had a "stalk" connecting them to the cell membrane. Deeper localized as well as paranuclear MLS floated in the cytoplasm without any connection with cytoplasmic membrane or adjacent intracellular structures (such as vacuoles or the nucleus). Intranuclear MLS were not observed.

Table 3 NHERF1/EBP50 immunoexpression in additional 12 cases (36 main samples) of clear cell RCCs

NHERF1/EBP50 immunostaining	Intensity	Number of samples based on WHO/ISUP nuclear grade			
		1	2	3	4
Lumen-like structures formation and density					
Membranous	0	0	2	9	0
	1+	0	3	5	2
	2+	0	1	3	1
	3+	3	3	4	0
Submembranous	0	0	0	10	0
	1+	0	3	4	2
	2+	0	3	1	1
	3+	3	3	6	0
Paranuclear	0	0	5	21	3
	1+	0	2	0	0
	2+	3	0	0	0
	3+	0	2	0	0

NHERF1, Na+/H+ exchanger regulatory cofactor 1; RCC, renal cell carcinoma; WHO/ISUP, World Health Organization/International Society of Urological Pathology.

Discussion

Clear cell and papillary RCCs arise from proximal tubular epithelial cells, while chromophobe RCC and oncocytoma arise from intercalated cells of the collecting duct. Despite the similarity of origin and function, each pathology has unique oncogenesis, molecular and IHC profiles, and behavior. Before becoming tumorous, all these cells perform many functions, the common of which is the exchange of Na^+/H^+ with the maintenance of an alkaline pH (28). In the proximal tubular cells of the kidney, the main Na^+/H^+-antiporter is NHE3, which is regulated by several cofactors, one of which is NHERF1 (29).

Primarily, working with sixty-six cases, including 14 (21%) oncocytomas and 52 (79%) RCCs (clear cell, papillary, and chromophobe types), we identified some type of abnormal NHERF1/EBP50 immunoexpression in most cases compared to benign kidney tissue (*Figure 2A-2D*). Only 5 cases of ccRCC and 4 cases of pRCC type I (total 14%) showed a normal staining pattern, but heterogeneity of expression was still observed with focal foci of complete loss of immunostaining.

Out of sixty-six cases, only 9 (14%) ccRCC cases were found to have unique intracytoplasmic MLSs of NHERF1/EBP50 immunocondensation. On light microscopy, they were dot-like (rarely tiny ring-shaped) and were observed between neighboring tumor cells and/or under the cell membrane or intracytoplasmic. The distribution of MLS was heterogeneous within individual tumors, as well as between different tumors, including tumor grades and stages. To identify the MLS by electron microscopy, fresh tumor tissue was required. Twelve additional cases of ccRCC were collected for further analysis, forming a group of 36 tumor samples (3 samples per case) (*Table 3*).

In these twelve additional cases of ccRCC, WHO/ISUP grades 1, 2, 3, and 4 were represented by 3 (8%), 9 (25%), 21 (58%), and 3 (8%) samples, respectively. Due to the observed heterogeneity in NHERF1/EBP50 immunoexpression, the composition of each sample was evaluated qualitatively.

The microlumen highlighted with NHERF1/EBP50 had a similar pattern to the initially studied ccRCC. In the hotspot areas, the detection of MLS formations exhibited variability, ranging from 1–2 to several or many per glass slide. Overall, MLS were detected in 28 (78%) samples and were most frequently seen in the WHO/ISUP low-grade sample group (combined grade 1 and 2 tumor samples) with statistical significance found for submembranous

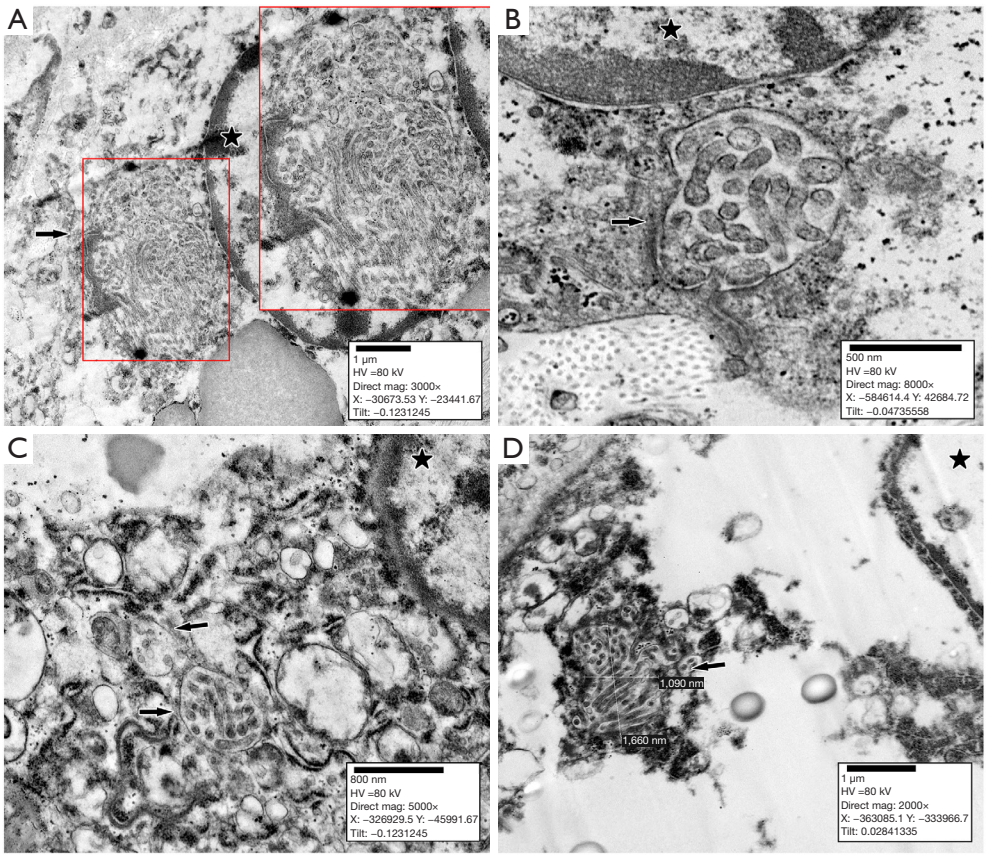

Figure 4 Transmission electron photomicrograph of microlumen-like structures with entrapped microvilli in paranuclear localizations in clear cell renal cell carcinoma cells. (A) An electron micrograph demonstrates the presence of microlumen-like structure (indicated by an arrow) adjacent to the nuclear karyolemma (marked by an asterisk). (B-D) Subsequent electron micrographs exhibit smaller microlumen-like structures (indicated by arrows) dispersed in the cytoplasm or positioned in close proximity to intracellular structures, specifically near the nuclei (indicated by asterisks). Images A, B, C represent case #11, while image D represents case #9.

and paranuclear localizations (P=0.0146 and P<0.0001, respectively) (*Figure 3*, *Table 3*). Out of the 36 samples, a total of 9 (25%) were chosen for TEM study. These selected samples included cases #1 (sample A), #2 (samples A and B), #3 (sample A), #7 (sample A), #8 (sample C), #9 (samples A and B), and #11 (sample A), as they exhibited the highest quantity of MLS.

Ultrastructural analysis of the samples revealed MLS in the form of thick microvilli, which were enclosed by a single-layer membrane (*Figures 4A-4D*,*5A-5D*). The membranous localization of MLS can be explained by the overgrowth of tumor cells and the loss of tubular organization, when the apical membranes of tumor cells begin to come into contact with each other, but do not completely disappear. With the submembranous location of MLS, in most cases, the "stalk" of the cell membrane was detected, attaching it to the overlying cell membrane. However, the intracytoplasmic and paranuclear localization of MLS has been difficult to explain, and the exact mechanism leading to this arrangement is still unknown, as is its effect on cell functionality. In some cases, the lack of connection with the cell membrane may probably be explained by the cut plane of the tissue.

In comparison to the previously published study on NHERF1/EBP50 expression in ccRCC, our cases exhibited weak, focal, and infrequent nuclear expression, which could be attributed to the difference in the antibodies used (23). Of the initial study group, only one case of ccRCC and two cases of pRCC type I demonstrated nuclear positivity in combination with membranous and cytoplasmic expression. For the additional 12 cases of ccRCC, nuclear immunostaining was weak and was observed in WHO/ISUP

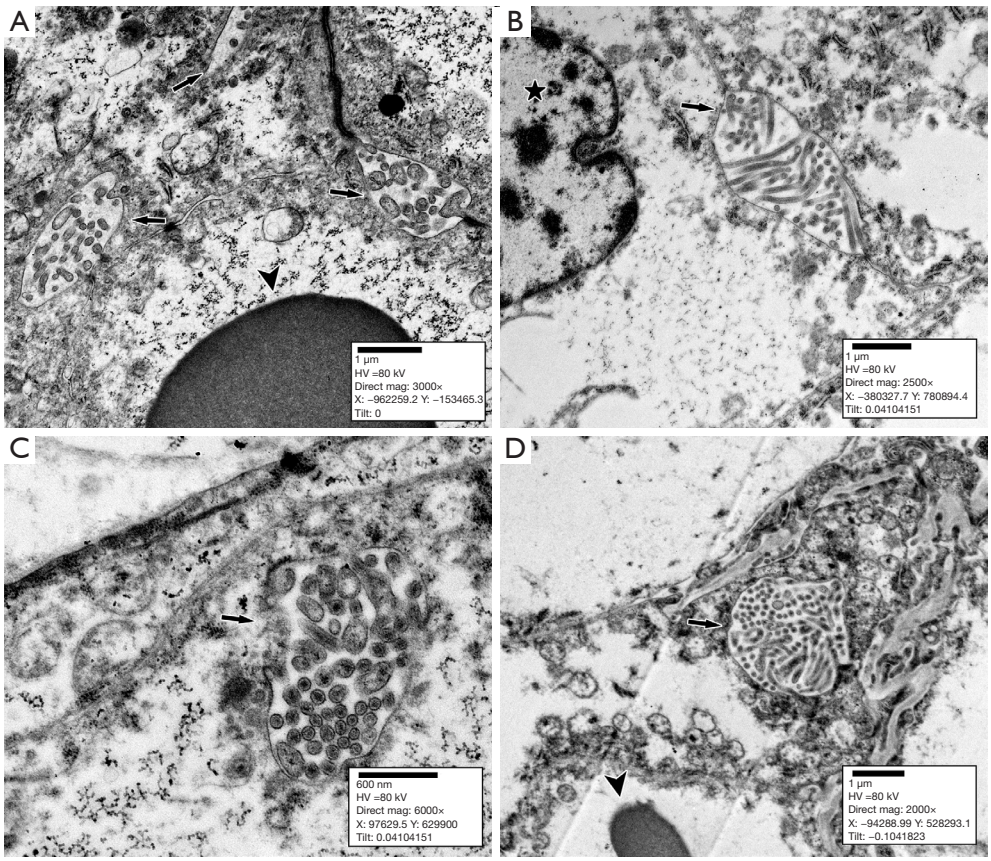

Figure 5 Transmission electron photomicrograph of microlumen-like structures with entrapped microvilli in membranous and submembranous localizations in clear cell renal cell carcinoma cells. (A,B) Electron micrographs unveil the presence of distinct microlumen-like structures (indicated by arrows) situating between two cells, with clearly defined cytoplasmic membranes extending on either side of these formations. Notably, the erythrocyte (indicated by an arrowhead) and the tumor cell nucleus (marked by an asterisk) are also visible. (C,D) Notably, submembranous microlumen-like structures (indicated by arrows) are observed, displaying no connection with the neighboring cell membranes or surrounding cytoplasmic structures. Erythrocytes (indicated by an arrowhead) are also seen. Image A represents case #1, while images B and C correspond to case #8. Lastly, image D corresponds to case #2.

grades 2 and 3 samples. However, intranuclear MLS were not seen on TEM. Tumor cells in close proximity to necrotic areas did not show MLS. In one case with necrosis and sarcomatoid features, only rare membranous MLS occurred.

Taking into account the data on the tumor suppressor function of NHERF1, this can be supported by our results (21). In areas of tubule formation by tumor cells, none of the studied samples had a bright luminal and diffuse cytoplasmic NHERF1/EBP50 immunopositivity, and in most cases it was completely absent. Moreover, our results are supported by the pro-oncogenic function of NHERF1/EBP50 (22). We tend to assume that MLSs translocated to the cytoplasm may play a role in the early stages of disease progression when cells have a low WHO/ISUP nuclear grade. However, upon reaching a higher nuclear grade, tumor cells begin to lose MLS, and their number completely disappears in the areas adjacent to necrosis.

MLS-forming NHERF1/EBP50 condensations were identified in the membranous, submembranous, and paranuclear regions by light microscopy. To date, these structures appear to be unique to ccRCC among other kidney tumors. We identified, examined, and presented them using NHERF1/EBP50 immunohistochemical and TEM. Our results may shed light on some mechanisms of oncogenesis in ccRCC and may prompt further research.

Undoubtedly, our work carries certain limitations. The sample size under study remains small, and the possibility of bias cannot be entirely disregarded. However, despite these

limitations, our study has successfully identified distinctive findings in ccRCC, elucidated the interconnections among the grouped samples, and presented novel insights that have not been extensively explored for these tumor types.

Additionally, it is important to note that we maintained the grouping of type I and II papillary RCC cases, as these diagnoses were assigned before the publication of the latest edition of the WHO Classification of Tumors (5th edition), which no longer includes this subdivision.

Furthermore, it is worth noting that the dimensions of microlumens may vary significantly, and it is important to consider the influence of the plane of sectioning on our measurements.

Conclusions

Neoplastic kidney disease continues to be a major cause of morbidity and mortality worldwide. RCC, in particular, is a heterogeneous group of malignant neoplasms of the kidneys, the frequency of which is steadily increasing every year (2,5). ccRCC is the most common histological type and is a well-known but understudied tumor. MLSs, which appear to be a unique feature of ccRCC among other types of RCC, have been found in membranous, submembranous, and paranuclear localizations. They are statistically more common among ccRCC with WHO/ISUP low-grade nuclear features.

Abnormal position of intracellular structures, changes in intra- and extracellular ion balance, formation of new structures—all these findings can help to understand oncogenesis of renal tumors, open up new therapeutic possibilities and, as a result, benefit the patient.

Acknowledgments

We would like to thank Mr. Corey Gemelli (Department of Pathology, Ochsner LSU Health, Shreveport, LA, USA) and our team of histotechnicians for their help with tissue processing and immunohistochemistry.
Funding: None.

Footnote

Reporting Checklist: The authors have completed the STROBE reporting checklist. Available at https://tau.amegroups.com/article/view/10.21037/tau-23-101/rc

Data Sharing Statement: Available at https://tau.amegroups.com/article/view/10.21037/tau-23-101/dss

Peer Review File: Available at https://tau.amegroups.com/article/view/10.21037/tau-23-101/prf

Conflicts of Interest: All authors have completed the ICMJE uniform disclosure form (available at https://tau.amegroups.com/article/view/10.21037/tau-23-101/coif). The authors have no conflicts of interest to declare.

Ethical Statement: The authors are accountable for all aspects of the work in ensuring that questions related to the accuracy or integrity of any part of the work are appropriately investigated and resolved. The study was conducted in accordance with the Declaration of Helsinki (as revised in 2013). The study was approved by the Institutional Review Board Committee at LSU Health Shreveport (No. CR00002192_STUDY00000740) and individual consent for this retrospective analysis was waived.

References

1. Siegel RL, Miller KD, Fuchs HE, et al. Cancer statistics, 2022. CA Cancer J Clin 2022;72:7-33.
2. Capitanio U, Bensalah K, Bex A, et al. Epidemiology of Renal Cell Carcinoma. Eur Urol 2019;75:74-84.
3. Nabi S, Kessler ER, Bernard B, et al. Renal cell carcinoma: a review of biology and pathophysiology. F1000Res 2018;7:307.
4. Young JR, Coy H, Douek M, et al. Clear Cell Renal Cell Carcinoma: Identifying the Loss of the Y Chromosome on Multiphasic MDCT. AJR Am J Roentgenol 2017;209:333-8.
5. Cairns P. Renal cell carcinoma. Cancer Biomark 2010;9:461-73.
6. Toth AT, Cho DC. Emerging Therapies for Advanced Clear Cell Renal Cell Carcinoma. J Kidney Cancer VHL 2020;7:17-26.
7. Verlander JW. Normal ultrastructure of the kidney and lower urinary tract. Toxicol Pathol 1998;26:1-17.

8. Jones DB. Scanning electron microscopy of basolateral surfaces of rat renal tubules isolated by sequential digestion. Anat Rec 1985;213:121-30.
9. Zhuo JL, Li XC. Proximal nephron. Compr Physiol 2013;3:1079-123.
10. Fliegel L. Structural and Functional Changes in the Na(+)/H(+) Exchanger Isoform 1, Induced by Erk1/2 Phosphorylation. Int J Mol Sci 2019;20:2378.
11. Stemmer-Rachamimov AO, Wiederhold T, Nielsen GP, et al. NHE-RF, a merlin-interacting protein, is primarily expressed in luminal epithelia, proliferative endometrium, and estrogen receptor-positive breast carcinomas. Am J Pathol 2001;158:57-62.
12. He P, Zhao L, No YR, et al. The NHERF1 PDZ1 domain and IRBIT interact and mediate the activation of Na+/H+ exchanger 3 by ANG II. Am J Physiol Renal Physiol 2016;311:F343-51.
13. Weinman EJ, Cunningham R, Wade JB, et al. The role of NHERF-1 in the regulation of renal proximal tubule sodium-hydrogen exchanger 3 and sodium-dependent phosphate cotransporter 2a. J Physiol 2005;567:27-32.
14. Weinman EJ, Steplock D, Wang Y, et al. Characterization of a protein cofactor that mediates protein kinase A regulation of the renal brush border membrane Na(+)-H+ exchanger. J Clin Invest 1995;95:2143-9.
15. Bushau-Sprinkle AM, Lederer ED. New roles of the Na(+)/H(+) exchange regulatory factor 1 scaffolding protein: a review. Am J Physiol Renal Physiol 2020;318:F804-8.
16. Sun L, Zheng J, Wang Q, et al. NHERF1 regulates actin cytoskeleton organization through modulation of α-actinin-4 stability. FASEB J 2016;30:578-89.
17. Bushau-Sprinkle A, Barati MT, Gagnon KB, et al. NHERF1 Loss Upregulates Enzymes of the Pentose Phosphate Pathway in Kidney Cortex. Antioxidants (Basel) 2020;9:862.
18. Leiphrakpam PD, Lazenby AJ, Chowdhury S, et al. Prognostic and therapeutic implications of NHERF1 expression and regulation in colorectal cancer. J Surg Oncol 2020;121:547-60.
19. Yang F, Hu M, Chang S, et al. Alteration in the sensitivity to crizotinib by Na(+)/H(+) exchanger regulatory factor 1 is dependent to its subcellular localization in ALK-positive lung cancers. BMC Cancer 2020;20:202.
20. Georgescu MM, Olar A, Mobley BC, et al. Epithelial differentiation with microlumen formation in meningioma: diagnostic utility of NHERF1/EBP50 immunohistochemistry. Oncotarget 2018;9:28652-65.
21. Vaquero J, Nguyen Ho-Bouldoires TH, Clapéron A, et al. Role of the PDZ-scaffold protein NHERF1/EBP50 in cancer biology: from signaling regulation to clinical relevance. Oncogene 2017;36:3067-79.
22. Yang Y, Liang J, Zhao C, et al. NHERF4 hijacks Mas-mediated PLC/AKT signaling to suppress the invasive potential of clear cell renal cell carcinoma cells. Cancer Lett 2021;519:130-40.
23. Lema BE, Patricio GM, Kreimann EL. Nuclear expression of NHERF1/EBP50 in Clear Cell Renal Cell Carcinoma. Acta Histochem 2021;123:151717.
24. Weinman EJ, Lakkis J, Akom M, et al. Expression of NHERF-1, NHERF-2, PDGFR-α, and PDGFR-β in Normal Human Kidneys and in Renal Transplant Rejection. Pathobiology 2002;70:314-23.
25. WHO Classification of Tumours Editorial Board. Urinary and male genital tumours [Internet]. Lyon (France): International Agency for Research on Cancer. vol (WHO classification of tumours series, 5th ed.; vol. 8). 2022 [cited 2023 May 11].
26. Xiao Q, Yi X, Guan X, et al. Validation of the World Health Organization/International Society of Urological Pathology grading for Chinese patients with clear cell renal cell carcinoma. Transl Androl Urol 2020;9:2665-74.
27. Moch H, Cubilla AL, Humphrey PA, et al. The 2016 WHO Classification of Tumours of the Urinary System and Male Genital Organs-Part A: Renal, Penile, and Testicular Tumours. Eur Urol 2016;70:93-105.
28. Cardone RA, Alfarouk KO, Elliott RL, et al. The Role of Sodium Hydrogen Exchanger 1 in Dysregulation of Proton Dynamics and Reprogramming of Cancer Metabolism as a Sequela. Int J Mol Sci 2019;20:3694.
29. Sarker R, Valkhoff VE, Zachos NC, et al. NHERF1 and NHERF2 are necessary for multiple but usually separate aspects of basal and acute regulation of NHE3 activity. Am J Physiol Cell Physiol 2011;300:C771-82.

Cite this article as: Aksionau A, Silva RA, Hartman B, Flowers A. NHERF1/EBP50 immunoexpression in renal cell carcinomas and oncocytomas with ultrastructural analysis of clear cell renal cell carcinoma. Transl Androl Urol 2023;12(8):1283-1295. doi: 10.21037/tau-23-101

